

UWED: Unsigned Distance Field for Accurate 3D Scene Representation and Completion

March 18, 2022

Jean Pierre Richa^{1,2}, Jean-Emmanuel Deschaud¹, François Goulette¹
and Nicolas Dalmaso²

¹ MINES ParisTech, PSL University, Centre for Robotics, 75006 Paris, France

² ANSYS France, 15 Pl. Georges Pompidou, 78180 Montigny-le-Bretonneux, France

Abstract

Scene Completion is the task of completing missing geometry from a partial scan of a scene. The majority of previous methods compute an implicit representation from range data using a Truncated Signed Distance Function (TSDF) on a 3D grid as input to neural networks. The truncation limits but does not remove the ambiguous cases introduced by the sign for non-closed surfaces. As an alternative, we present an Unsigned Distance Function (UDF) called Unsigned Weighted Euclidean Distance (UWED) as input to the scene completion neural networks. UWED is simple and efficient as a surface representation, and can be computed on any noisy point cloud without normals. To obtain the explicit geometry, we present a method for extracting a point cloud from discretized UDF values on a regular grid. We compare different SDFs and UDFs for the scene completion task on indoor and outdoor point clouds collected from RGB-D and LiDAR sensors and show improved completion using the proposed UWED function.

1 Introduction

Distance functions computed on 3D regular grids provide rich information about the geometry of a scene. Many distance functions have been proposed to tackle a wide variety of tasks, such as surface reconstruction [21, 49], Simultaneous Localisation And Mapping (SLAM) [15, 31], path planning [32] and scene completion [11, 39]. Traditional surface reconstruction methods [10, 21, 24] compute a Signed Distance Function (SDF) representation from range images or point clouds on a regular volumetric grid. A zero level set extraction algorithm such as Marching Cubes [27] can be deployed to extract the final mesh with geometric details proportional to the grid resolution, and a trade-off between a fine

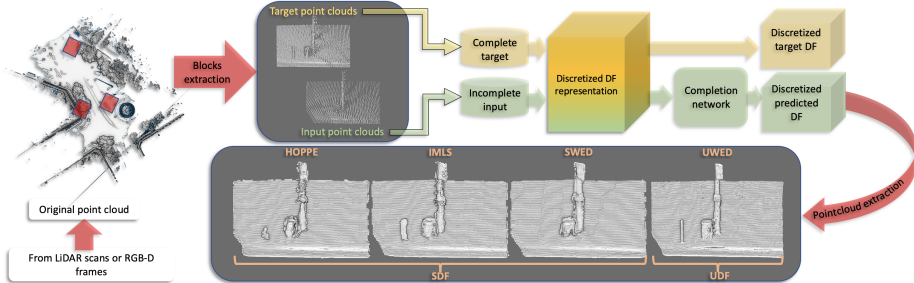


Figure 1: Self-supervised 3D scene completion comparing several Signed Distance Functions (SDFs) and Unsigned Distance Functions (UDFs). Small point cloud blocks are extracted from the original point cloud; random frames (for RGB-D) or scans (for LiDAR) are removed for the input, while all of the points are used for the target. All point clouds are later transformed into distance function representations on discretized grids; then, the network is trained to learn the completion of the representations. Our Unsigned Weighted Euclidean Distance (UWED) function eliminates the sign ambiguities resulting from SDFs while achieving higher accuracy on the scene completion task.

resolution and computational complexity is inevitable. These methods fill small holes by local interpolation, but they fail to fill large missing areas resulting from occluded regions caused by the foreground, dynamic objects, or from the high sparsity of points.

With advances in learning-based methods, recent studies have looked to develop approaches tackling the problem of larger missing areas, which gave rise to the scene completion task. Different data representations have been proposed that focus primarily on 3D binary occupancy grids, point clouds, or implicit functions representing the underlying surface. Occupancy voxel grids do not allow the geometry to be finely represented [12, 13]. Performing point cloud completion like PCN [44] or more recently VRC-Net [33] are limited to single objects and are not able to deal with large scenes. On the contrary, implicit surface representation using Truncated Signed Distance Function (TSDF) has proven to be able to accurately represent and predict the geometry of large scenes [5, 6, 11, 13, 14, 20, 39, 46].

There are also reconstruction methods where the geometry is encoded into neural networks, such as Occupancy Network [28], DeepSDF [34] or unsigned geometric data in SAL [2] and DUDE [41], but these fully-connected network architectures generalize poorly to unseen data and cannot be applied to large 3D scenes.

One major issue in using SDFs to implicitly represent the underlying 3D surface is their need to perform inside/outside classification of the volume. For point clouds, such as those obtained from real-world scenes, this issue can be solved by computing point-wise oriented normal estimation (which is a challenging task when done on noisy point clouds [29, 38]) and using the normals to

infer the sign. Truncating the SDF values results in a Truncated (T)SDF that limits the interference between spatially nearby surfaces and the dilation of the geometry on the boundaries of surfaces. However, TSDF does not eliminate the geometry dilation and results in many artifacts (see 3D example in Figure 1 and 2D example in Figure 2).



Figure 2: A 2D example of an open surface (non-closed surface). Signed distance functions (SDF) do not handle open surfaces, and even if the truncation limits the side effects, the extraction to point clouds will generate border effects. Using an unsigned distance function (UDF), eliminates the problem of negative and positive sides. However, the difficulty lies in the extraction of a point cloud. Here, the point clouds extraction from SDF and UDF follows the methods described in section 3.2. We also show flipped versions of TSDF and TUDF that remove strong gradients at truncation distance.

To address these issues, we propose the computation of an Unsigned Distance Function (UDF) on a 3D volumetric grid directly from point clouds, which can then be applied on scenes acquired using RGB-D or LiDAR sensors. However, the extraction of an explicit geometry such as a mesh from a UDF is difficult [9]. Thus, we present a method for extracting point clouds from unsigned distance fields. We show that our unsigned distance representation allows the completion network to better understand the scene’s geometry (without managing the sign) and therefore predicts a better completion of the scene.

Our contributions are summarized as follows:

- A fast and robust unsigned distance function, UWED, for scene representation.
- A method to extract a point cloud from an unsigned distance field computed on a 3D regular grid.
- Extensive comparisons of scene completion using UWED and several other distance functions as implicit scene representations for various environments (indoor and outdoor) and sensors (RGB-D and LiDAR).

2 Related Work

Signed Distance Functions Using distance functions on 3D volumetric grids for surface reconstruction traces back to the seminal work of Hoppe *et al.* [21],

in which a Signed Distance Field $\phi : \mathbb{R}^3 \rightarrow \mathbb{R}$ was used to implicitly represent the underlying surface from a point cloud:

$$\phi(x) = \mathbf{n}_i \cdot (x - \mathbf{p}_i) \quad (1)$$

where x is the voxel coordinates in the 3D grid, \mathbf{p}_i is the nearest neighbor of \mathbf{x} in the point cloud P , and \mathbf{n}_i is the normal unit vector associated with the point \mathbf{p}_i .

Having computed the SDF on a 3D regular grid, the Marching Cubes algorithm [27] extracts the final iso-surface as a mesh.

Following this pioneering work, several methods were proposed to deal with noisy data, such as Implicit Moving Least Squares (IMLS) [24], which approximates the local neighborhood of a given voxel in the grid as a weighted average of the local point functions.

In a different approach, the volumetric fusion method of VRIP [10] takes advantage of range images by meshing the depth image to cast a ray from the sensor origin to the voxel of the volumetric grid, obtaining a signed distance to the mesh, and then merges the scans distances in a least-squares sense. However, this distance function can only be computed from range images and cannot be used directly on point clouds.

Other surface reconstruction methods [22, 23] use global implicit functions such as indicator functions where the reconstruction problem is solved using a Poisson system equation, others use 3D Delaunay tetrahedralization [3, 25, 47] and more recently applying 3D ConvNets [35, 40].

However, all these methods attempt to produce watertight meshes. In case of real-world scenes with open shapes, a truncation on the computation of SDFs can help but still produce artifacts (see Figure 2).

Unsigned Distance Functions UDFs solve the ambiguity introduced by SDFs, because they eliminate the need to define an interior and exterior. However, it is difficult to extract a well-behaved final mesh from such functions. One work [9] proposes a variant of the Marching Cubes to be used on an unsigned distance field, but the method results in holes in the reconstructed final mesh. Another work [30] attempts to obtain a consistent signed distance field from unsigned distances on the discretized grid, but this approach comes with the drawback of a high computational cost, not scalable to large scenes. SAL [2] trains a fully-connected network to infer the sign of a distance function from unsigned data but shows this only on object-level data. NDF [8] and DUDE [41] learn a volumetric unsigned distance encoded in a neural network. NDF extract a dense point cloud by projecting points using the gradient field from the back-propagation through the network, while DUDE also learns a normal vector field along with the distance function. However, the representation of the scene through a neural network limits the size of the scene.

Scene completion The increased availability of range sensors and advances in learning-based algorithms have made it possible to obtain large amounts of data

and train neural networks to predict larger missing areas caused by occlusions from the foreground and dynamic objects. Two main approaches to geometry completion exist in the literature. Object-level completion [12, 43, 44] focuses on the completion of single objects, such as chairs, cars, and tables, but they do not scale to large scenes, which limits their use to simple objects. Scene-level completion overcomes the shape completion limitation and tries to complete the missing geometry in large scenes.

Scene completion from RGB-D sensors Scene completion from a single depth image was introduced to complete missing scenes in indoor settings with SSCNet [39]. This paved the way for completion beyond traditional surface reconstruction methods, which increased the interest in the scene completion task [42, 45]. These earliest works focused on completing the scene from a single depth image and used a TSDF as their scene representation, with TSDF being the signed distance to the closest point on the surface, similar to the implicit representation of Hoppe *et al.* [21]. They used a flipped version of the TSDF to remove discontinuities around the truncation of the function and get strong gradients around the surface, giving more signal to the network around the surface enabling it to better learn the geometry. When multiple range images are available, such as in Matterport3D [4], most methods use the volumetric fusion VRIP [10] to obtain the discretized TSDF representation of the scene. They also use different network architectures to infer the missing geometry. For instance, ScanComplete [13] uses a U-Net architecture on dense volumes, and SG-NN [11] uses a U-Net with sparse convolutions. In our work, we leverage this last network architecture, SG-NN, to evaluate the performance of different distance function representations. Some works perform semantic scene completion (survey in [36]), in which they complete the scene, while predicting per-voxel semantic class as well, such as with ScanComplete [13]. Others predict color information such as in SPSG [14] (which is an extension of SG-NN [11]). Our work focuses on improving the geometry representation, but could be easily integrated with these works by adding semantic or color information.

Scene completion from LiDAR sensors Fewer works were done on scene completion from LiDAR point clouds. LMSCNet [37] proposes a lightweight 2D U-Net backbone that is used on the x, y dimensions to reduce the computation complexity and complete a scene from a single LiDAR frame. This method provides fast inference, but is not optimal for accurate geometry prediction since the input is an occupancy grid. Another work [7] performs Bird’s Eye View (BEV) projection and extracts sparse 2D features along the x-y plane to perform depth completion, they subsequently extract 3D normal information, which is later used to compute the TSDF values on a 3D regular grid. The inference of the network is also a 3D occupancy grid. However, previous works [12, 13] have shown that the use of implicit functions (TSDF) allows better learning of geometry than the use of occupancy grids.

3 Unsigned Distance Function

In this section, we present our UDF for implicit scene representation and how we can extract an explicit geometry as point clouds from UDFs.

3.1 Our Unsigned Weighted Euclidean Distance (UWED)

Our UDF can be directly computed on any point cloud, without the need for normals estimation. Since using the distance to the nearest neighbor results in a noisy distance measurement to the surface, especially when computed on noisy data such as point clouds from LiDAR, we compute a weighted average of distances. To weight the contribution of each point in the neighborhood as a function of its distance, we use a Gaussian kernel and call our distance function representation Unsigned Weighted Euclidean Distance (UWED):

$$\text{UWED}(x) = \frac{\sum_{\mathbf{p}_k \in N_x} \|x - \mathbf{p}_k\|_2 \theta_k(x)}{\sum_{\mathbf{p}_k \in N_x} \theta_k(x)} \quad (2)$$

where x is the voxel coordinates, N_x is the set of \mathbf{p}_k neighboring points from x in the point cloud P , and θ_k is the Gaussian weight defined as:

$$\theta_k(x) = e^{-\|x - \mathbf{p}_k\|_2^2 / \sigma^2} \quad (3)$$

where σ is a parameter of the influence of points in the neighborhood. N_x can then be approximated as a sphere of center x and radius 3σ .

We can see that our UWED function does not require normal information, which greatly reduces the computational cost compared to SDFs. UWED is very close to the classical IMLS function [24]:

$$\text{IMLS}(x) = \frac{\sum_{\mathbf{p}_k \in N_x} \mathbf{n}_k \cdot (x - \mathbf{p}_k) \theta_k(x)}{\sum_{\mathbf{p}_k \in N_x} \theta_k(x)} \quad (4)$$

where IMLS is a weighted average of the point-to-plane distances (as in Hoppe [21]), and UWED is a weighted average of the euclidean distances.

Our formulation results in a smooth function that is robust in the presence of noisy data, which is the case in real-world datasets from RGB-D sequences or LiDAR acquisitions.

After obtaining UWED computed on a 3D regular grid, we convert the values into voxel units and truncate the function at 3 voxels (like in [11,13]), obtaining the Truncated (T)UWED on a sparse 3D grid.

Our experiments show that we obtain better geometry-learning ability by flipping our UWED function as in [39]: $f\text{-}(T)\text{UWED}(x) = 3 - (T)\text{UWED}(x)$. We get smoother gradients between the TUDF values and empty space in the sparse grid by overcoming the discontinuity of the function at truncation distance (visible in Figure 2).

3.2 Point cloud extraction from SDFs and UDFs

Once the point cloud is transformed into an SDF or UDF on a sparse grid, the scene completion neural network (after being trained) predicts a new SDF or UDF (representing the completed geometry of the scene). We first show how a point cloud can be extracted from an SDF, similar to extracting meshes from Marching Cubes [27]. We will then explain our method for extracting a point cloud from a UDF.

Extracting an explicit geometry in the form of a point cloud makes it possible to compare the results directly with the original data, which is also a point cloud (unlike a mesh-to-mesh comparison where the ground truth mesh is constructed by meshing the original point cloud). Point clouds are also a good geometry proxy: it is an easy representation to exploit because no topology has to be considered. They can also directly be used for rendering with methods such as Splatting [48] or more recent works such as Neural Point-Based Graphics [1].

3.2.1 Point cloud extraction from SDF

Marching Cubes [27] is a method widely used for extracting a mesh from a signed distance field. However, it is also possible to use the same technique to extract a point cloud instead of a mesh. A point cloud can be obtained from an SDF computed on a regular grid, by linearly interpolating a 3D point using the SDF values on each edge between two consecutive voxels having opposite SDF signs. The point cloud created corresponds exactly to the vertices of the mesh extracted using Marching Cubes [27]. In our experiments, we use this method for point cloud extraction from the different SDFs.

3.2.2 Our proposed method of point cloud extraction from UDF

We propose here a method for extracting a high-quality point cloud from an unsigned distance field. We devise candidate selection criteria to check if an occupied voxel should be used to extract a point. For each occupied voxel $\mathbf{v}_{i,j,k}$ in the discretized grid, we check the UDF value of the current voxel $\text{udf}_{i,j,k}$ and the six neighboring voxels on the x, y, and z axes. If all UDF values are defined (some voxels may not have UDF values because we are using sparse grids), and the UDF value of the current voxel is between $1 < \text{udf}_{i,j,k} < 3$ in voxel units, then it is selected as a candidate for extraction. The condition $\text{udf}_{i,j,k} > 1$ guarantees that all edges between the current voxel and its six neighboring voxels do not cross the surface.

We then compute an approximation of the gradient of the unsigned distance field with finite differences and get the unit direction vector as follows:

$$\mathbf{g}_{i,j,k} = \begin{bmatrix} \text{udf}_{i+1,j,k} - \text{udf}_{i-1,j,k} \\ \text{udf}_{i,j+1,k} - \text{udf}_{i,j-1,k} \\ \text{udf}_{i,j,k+1} - \text{udf}_{i,j,k-1} \end{bmatrix}, \mathbf{d}_{i,j,k} = \frac{\mathbf{g}_{i,j,k}}{\|\mathbf{g}_{i,j,k}\|} \quad (5)$$

We obtain the coordinates of the new extracted point on the surface by projection, through the use of the UDF value at the current voxel and the

estimated direction vector:

$$\mathbf{p}_{new} = \mathbf{v}_{i,j,k} - v_size \text{ udf}_{i,j,k} \mathbf{d}_{i,j,k} \quad (6)$$

where $\mathbf{v}_{i,j,k}$ is the 3D coordinates of the current voxel, v_size is the voxel size and $\text{udf}_{i,j,k}$ is the scalar unsigned distance in voxel units.

This method does not need the sign to find the surface and extracts better point clouds than those extracted from SDFs, as shown in the experiments section.

Finally, if a mesh is required as the explicit surface representation, we can apply meshing techniques such as Screened Poisson [23] on the new, more complete, point cloud of the scene (but it will result in geometry dilation on open surfaces).

4 Experiments and Results

We claim that our UWED representation improves the scene completion task and helps the neural network better understand the geometry of the scene. For the network, we use a classic U-Net architecture (taken from SG-NN [11]) with sparse convolutions (SparseConvNet from [19]). As input to the network, we use the different distance function representations (signed and unsigned) and compare the predicted SDFs and UDFs. We use the proposed extraction methods explained in section 3.2 to obtain the final predicted point clouds that are compared to the target point clouds. We provide quantitative and qualitative results on the scene completion task, and for this, we experiment on a wide variety of scene point clouds, including real indoor scenes from RGB-D sensors using Matterport3D [4], synthetic outdoor scenes from a simulated LiDAR using CARLA simulator [17] that we call PC3D-CARLA and outdoor scenes from a real mobile LiDAR system that we call PC3D-Paris. For the synthetic and real outdoor datasets, we use the Paris-CARLA-3D (PC3D) dataset [16].

4.1 Distance Functions for Scene Completion

We compare six distance functions which consist of signed and unsigned versions of using the point-to-plane distance to the nearest neighbor (Hoppe [21]), the weighted average of the point-to-plane distances in a given neighborhood radius (IMLS [24]), and our proposed function.

For SDFs, we compare Hoppe [21], IMLS [24] and Signed Weighted Euclidean Distance (SWED), which is the signed version of UWED, using IMLS for the sign and computed as follows: $\text{SWED}(x) = \text{sign}(\text{IMLS}(x)) \text{ UWED}(x)$.

After obtaining the different SDFs, we convert them into voxel units and truncate the values at 3 voxels.

For the UDFs, we test several functions in order to have a complete comparison with our proposed UDF. Specifically, we use the unsigned versions of the SDFs, obtaining UHoppe, UIMLS, and UWED, where UWED is the UDF

introduced in section 3.1. Then, we convert them into voxel units and truncate the values at 3 voxels.

We do not use robust variants of SDFs such as FSS [18] or RIMLS [49] because they require more parameters (unlike all the functions tested, which have at most one parameter σ) as the objective is to show the advantage of using euclidean unsigned distances. We leave the use of more robust variants to future works.

First proposed in [39], a flipped version of TSDF for completing partial scans, flips the function to remove strong gradients at truncation distance from the surface and give more signal to the network near the surface. Thus, we include the non-flipped and flipped versions of all the distance functions in the comparisons.

For notation simplification, we remove the T from the SDF and UDF names, but all tested distance functions are truncated at 3 voxels and are defined on sparse 3D grids.

4.2 Datasets Preparation

We tested the different distance function representations and scene completion on three different datasets, namely, Matterport3D [4] (RGB-D frames in indoor environments), PC3D-CARLA (mobile LiDAR simulated in the virtual simulator CARLA [17]) and PC3D-Paris [16] (mobile LiDAR in real outdoor environments). These three datasets provide a wide variety of point clouds (indoor and outdoor environments), noise types (RGB-D and LiDAR sensor) with synthetic and real data.

To effectively evaluate the different distance functions on real data where we do not have ground truth, we follow the work done in SG-NN [11] where a percentage of data is removed in order to create incomplete point clouds for the network input and all of the points are used for the target point clouds (see Figure 1).

To split the datasets, we use the original Matterport3D and PC3D splits train/val/test. We remove 50 % of RGB-D frames and 90 % of LiDAR scans to build an incomplete input point cloud, compute the SDF or UDF values from it, and try to predict a new SDF or UDF using the DFs values computed on the original point cloud as the target.

For Matterport3D, we first convert the RGB-D frames into point clouds and keep the sensor positions to re-orient the computed normals needed for the SDFs. We extract 30 point cloud blocks from each room, which results in 12,000 point clouds (64x64x128 grid size with voxel size 2 cm) for training. The test set is composed of 6,000 point clouds from test set rooms.

For PC3D-CARLA, we extract 3,000 small blocks (128x128x128 grid size with voxel size 5 cm) from each of the four training towns (T_2 , T_3 , T_4 , T_5), resulting also in 12,000 point cloud blocks for training. The test set is composed of 6,000 point clouds from towns T_1 and T_7 .

We follow the same procedure for PC3D-Paris with 2,000 training point cloud blocks (128x128x128 grid size with voxel size 5 cm) from S_1 and S_2 . For

PC3D-Paris, we use only the S_3 test set, as S_0 contains vegetation that does not make sense for surface reconstruction. As a result, the test set is composed of 1,000 point clouds.

We use data augmentation strategies such as random rotations around z, random scalings between 0.8 and 1.2, and local noise additions.

For all the datasets, we compute the different distance functions on a regular grid, convert the values into voxel units and truncate the function at 3 voxels. As in SG-NN [11], we decrease the resolution by a factor of two each time to generate 4 hierarchical levels.

4.3 Metrics for Scene Completion

Previous works such as ScanComplete [13] or SG-NN [11] using TSDFs for the scene completion task compute the ℓ_1 distance between the predicted TSDF and the target TSDF. In SG-NN, “unsigned distances are used in the error computation to avoid sign ambiguity.” However, for an SDF, the sign is important for surface extraction (iso-zero). We cannot easily compare ℓ_1 results between signed and unsigned distances and accross functions.

As we are extracting point clouds from the predicted SDFs and UDFs (section 3.2), we can directly compare the extracted point cloud with the target cloud (which is the original raw point cloud). The most often used metric for comparing point clouds is the Chamfer Distance (CD) between the predicted P_1 and original P_2 point clouds:

$$CD = \frac{1}{2|P_1|} \sum_{x \in P_1} \min_{y \in P_2} \|x - y\|_2 + \frac{1}{2|P_2|} \sum_{y \in P_2} \min_{x \in P_1} \|y - x\|_2 \quad (7)$$

4.4 Implementation Details

We train the SG-NN network on an NVIDIA GeForce RTX 2070 SUPER. As in SG-NN, the loss is a combination of Binary Cross Entropy (BCE) on occupancy and ℓ_1 loss on SDF or UDF prediction. The trainings were done for 5 epochs for Matterport3D and PC3D-CARLA and 10 epochs for PC3D-Paris because the dataset is smaller (training time is around 24h for Matterport3D, 24h for PC3D-CARLA and 10h for PC3D-Paris) with ADAM optimizer, a learning rate of 0.001, a batch size of 8 and 1,000 iterations per hierarchical level for Matterport3D and PC3D-CARLA and 250 iterations for PC3D-Paris.

The parameter σ for the distance functions IMLS, SWED, UIMLS, and UWED (σ allows to be robust to noise) is fixed to 2 voxel size for all datasets. For distance functions that require normal computation on the point clouds (all except UWED), we estimate the normal at each point using PCA with $n = 30$ neighbors and obtain a consistent orientation using the RGB-D or LiDAR sensor position provided with the points.

4.5 Results of Distance Functions for Scene Representation

Before comparing the influence of distance functions on the scene completion network, we evaluate the capacity of the different implicit representations by computing the error introduced from passing through the different representations: point cloud \rightarrow DF \rightarrow point cloud. We then compute the CD between the original point cloud and the point clouds extracted from the different distance fields. We used the test sets of the three datasets with 6,000 point cloud blocks for Matterport3D, 6,000 point cloud blocks for PC3D-CARLA, and 1,000 point cloud blocks for PC3D-Paris. We compute the mean CD over all point clouds.

Figure 3 shows the qualitative results of these comparisons. We can see that Hoppe is very noisy (only exploiting the closest point) and that Hoppe and IMLS expand the geometry at the borders. This is clearly visible on the stair bar for Matterport, the street lamp in the CARLA synthetic data, and the window jamb for the Paris data. On the contrary, with our unsigned distance function UWED, we extract a geometry in the form of a point cloud that is very close to the original cloud.

This is verified quantitatively. Table 1 shows the mean CD results on the three datasets. We can see that our point clouds extraction from UWED is always better for all datasets.

Table 1: Results of computing the different distance functions on a regular grid for three datasets and then extracting the point clouds. We report the mean Chamfer Distance (in cm) between the extracted point clouds and the original ones, to compare the accuracy of each function without passing through the scene completion network inference.

Datasets	SDFs			UDFs		
	Hoppe	IMLS	SWED	UHoppe	UIMLS	UWED
Matterport3D	0.9 cm	0.82 cm	0.81 cm	0.8 cm	0.74 cm	0.6 cm
PC3D-CARLA	1.80 cm	1.78 cm	1.97 cm	1.67 cm	1.68 cm	1.62 cm
PC3D-Paris	2.41 cm	2.37 cm	2.44 cm	2.90 cm	2.72 cm	2.15 cm

4.6 Results of Distance Functions for Scene Completion

We compare the six distance functions on the three datasets with the non-flipped and flipped variants, which results in 36 trainings of SG-NN. All the quantitative results are visible in Table 2. We present the mean CD across all test sets of the three datasets (6,000 for Matterport3D, 6,000 for PC3D-CARLA, and 1,000 point clouds for PC3D-Paris). We can see that our UWED representation (flipped version) results in a lower CD for all datasets.

We can note from Table 2 that flipping the distance functions systematically improves results for UWED but not necessarily for SDFs. Indeed, for SDFs, the



Figure 3: Comparison of different implicit functions representations. From point clouds, we compute Signed Distance Functions (Hoppe and IMLS) or our Unsigned Distance Function (UWED), then we extract back a point cloud (without completion) to compare the accuracy of the extracted point clouds to the original point cloud. With UWED, we are able to extract smooth point clouds: the advantages can be seen all over the extracted point clouds, such as on the stair bar in Matterport and the window in the Paris dataset (Hoppe and IMLS dilate the geometry because of the sign and point-to-plane distance functions).

flipped function removes the discontinuity at the truncation distance and gets stronger gradients around the surface. However, it introduces a discontinuity at the surface level (iso-zero).

Figures 4, 5, and 6 show qualitative results for Hoppe, IMLS, and UWED distance functions (all flipped versions), on the test sets of the three datasets. We can see each time that higher quality point clouds are obtained after scene completion using our UWED representation (visible on stairs, trash can, and bollards). UWED is also able to complete larger missing regions (see the middle example in Figure 6).

Table 2: Scene completion results for different SDFs and UDFs on three datasets: Matterport3D (RGB-D frames in indoor), PC3D-CARLA (mobile LiDAR in virtual CARLA simulator), and PC3D-Paris (mobile LiDAR in outdoor urban scene). Results are the mean Chamfer Distance computed over the test sets of the three datasets (6,000, 6,000, and 1,000 points clouds, respectively).

	Matterport3D		PC3D-CARLA		PC3D-Paris	
	SDFs					
	non-flipped	flipped	non-flipped	flipped	non-flipped	flipped
Hoppe	1.54 cm	1.53 cm	6.32 cm	6.14 cm	7.62 cm	7.53 cm
IMLS	1.52 cm	1.51 cm	6.10 cm	6.09 cm	7.48 cm	7.56 cm
SWED	1.52 cm	1.54 cm	6.06 cm	6.19 cm	7.57 cm	7.54 cm
	UDFs					
	non-flipped	flipped	non-flipped	flipped	non-flipped	flipped
UHoppe	1.25 cm	1.26 cm	15.24 cm	6.00 cm	9.95 cm	7.96 cm
UIMLS	1.27 cm	1.32 cm	7.76 cm	6.68 cm	9.47 cm	7.73 cm
UWED	1.23 cm	1.22 cm	6.28 cm	5.73 cm	7.45 cm	7.27 cm

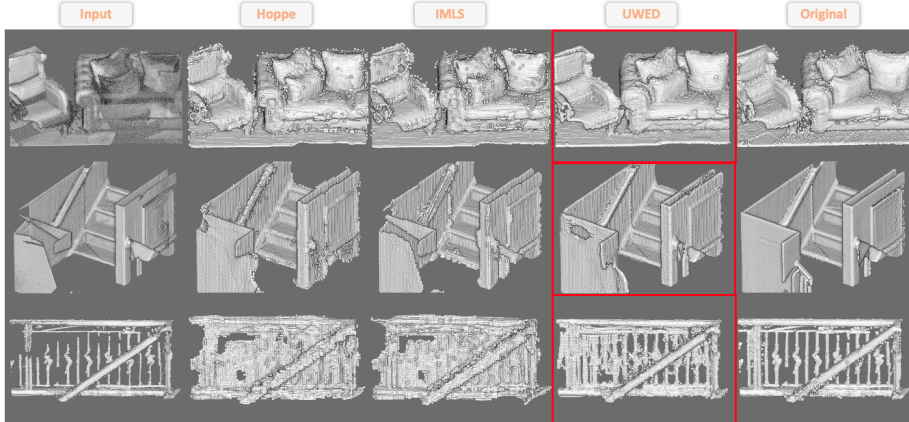


Figure 4: Scene completion inference using Hoppe, IMLS, and our UWED distance function on the Matterport3D test set (input has 50% of the original points).

4.7 Limitations and Perspectives

The main limitation of our UWED representation is that it does not allow the direct extraction of a mesh (unlike SDFs). However, it is possible to imagine

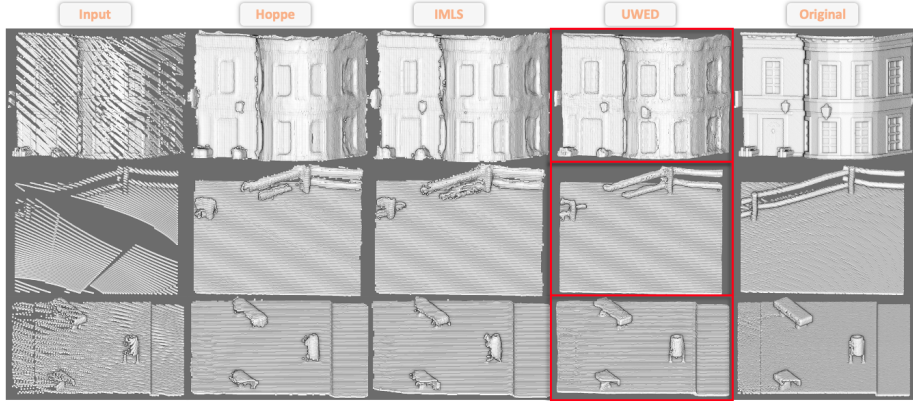


Figure 5: Scene completion inference using Hoppe, IMLS, and our UWED distance function on the PC3D-CARLA test set (input has 10% of the original points).

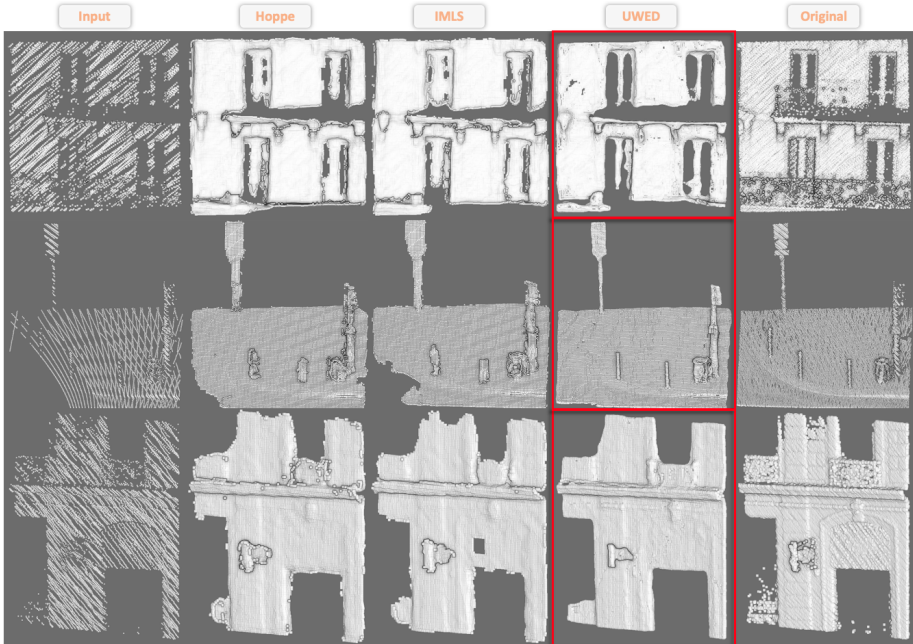


Figure 6: Scene completion inference using Hoppe, IMLS, and our UWED distance function on the PC3D-Paris test set (input has 10% of the original points).

a learning-based method that allows the inference of a mesh directly from an unsigned distance field, as inspired by Deep Marching Cubes [26].

In perspective, our UWED function showed excellent performance as scene

representation and in the scene completion task. Furthermore, this representation of 3D geometry seems to allow neural networks to learn geometry better. Thus, it should be possible to use this same representation for other tasks in 3D.

5 Conclusion

We presented an unsigned distance function for 3D scene representation that improves the quality of the completion task. We also introduced a point cloud extraction algorithm from an UDF computed on a sparse grid. Finally, we compared six different SDFs and UDFs on three different datasets. Our experiments showed quantitatively and qualitatively that our UWED implicit scene representation achieves the best completion results.

References

- [1] Aliev, K.A., Sevastopolsky, A., Kolos, M., Ulyanov, D., Lempitsky, V.: Neural point-based graphics. In: Vedaldi, A., Bischof, H., Brox, T., Frahm, J.M. (eds.) Computer Vision – ECCV 2020. pp. 696–712. Springer International Publishing, Cham (2020)
- [2] Atzmon, M., Lipman, Y.: Sal: Sign agnostic learning of shapes from raw data. In: 2020 IEEE/CVF Conference on Computer Vision and Pattern Recognition (CVPR). pp. 2562–2571 (2020). <https://doi.org/10.1109/CVPR42600.2020.00264>
- [3] Caraffa, L., Marchand, Y., Brédif, M., Vallet, B.: Efficiently distributed watertight surface reconstruction. In: 2021 International Conference on 3D Vision (3DV). pp. 1432–1441 (2021). <https://doi.org/10.1109/3DV53792.2021.00150>
- [4] Chang, A., Dai, A., Funkhouser, T., Halber, M., Niebner, M., Savva, M., Song, S., Zeng, A., Zhang, Y.: Matterport3d: Learning from rgb-d data in indoor environments. In: 2017 International Conference on 3D Vision (3DV). pp. 667–676 (2017). <https://doi.org/10.1109/3DV.2017.00081>
- [5] Chen, R., Huang, Z., Yu, Y.: Am2fnet: Attention-based multiscale and multi-modality fused network. In: 2019 IEEE International Conference on Robotics and Biomimetics (ROBIO). p. 1192–1197. IEEE Press (2019). <https://doi.org/10.1109/ROBIO49542.2019.8961556>
- [6] Chen, Y.T., Garbade, M., Gall, J.: 3d semantic scene completion from a single depth image using adversarial training. In: 2019 IEEE International Conference on Image Processing (ICIP). pp. 1835–1839 (2019). <https://doi.org/10.1109/ICIP.2019.8803174>
- [7] Cheng, R., Agia, C., Ren, Y., Li, X., Liu, B.: S3cnet: A sparse semantic scene completion network for lidar point clouds. CoRR **abs/2012.09242** (2020), <https://arxiv.org/abs/2012.09242>
- [8] Chibane, J., Mir, A., Pons-Moll, G.: Neural unsigned distance fields for implicit function learning. In: Advances in Neural Information Processing Systems (NeurIPS) (December 2020)
- [9] Congote, J., Moreno, A., Barandiaran, I., Barandiarán, J., Posada, J., Ruiz, O.E.: Marching cubes in an unsigned distance field for surface reconstruction from unorganized point sets. In: GRAPP (2010)
- [10] Curless, B., Levoy, M.: A volumetric method for building complex models from range images. In: Proceedings of the 23rd Annual Conference on Computer Graphics and Interactive Techniques. p. 303–312. SIGGRAPH '96, Association for Computing Machinery, New York, NY,

USA (1996). <https://doi.org/10.1145/237170.237269>, <https://doi.org/10.1145/237170.237269>

- [11] Dai, A., Diller, C., Niessner, M.: Sg-nn: Sparse generative neural networks for self-supervised scene completion of rgbd scans. In: 2020 IEEE/CVF Conference on Computer Vision and Pattern Recognition (CVPR). pp. 846–855 (2020). <https://doi.org/10.1109/CVPR42600.2020.00093>
- [12] Dai, A., Qi, C.R., Nießner, M.: Shape completion using 3d-encoder-predictor cnns and shape synthesis. In: 2017 IEEE Conference on Computer Vision and Pattern Recognition (CVPR). pp. 6545–6554 (2017). <https://doi.org/10.1109/CVPR.2017.693>
- [13] Dai, A., Ritchie, D., Bokeloh, M., Reed, S., Sturm, J., Nießner, M.: Scancomplete: Large-scale scene completion and semantic segmentation for 3d scans. In: 2018 IEEE/CVF Conference on Computer Vision and Pattern Recognition. pp. 4578–4587 (2018). <https://doi.org/10.1109/CVPR.2018.00481>
- [14] Dai, A., Siddiqui, Y., Thies, J., Valentin, J., Nießner, M.: Spsg: Self-supervised photometric scene generation from rgbd scans. In: 2021 IEEE/CVF Conference on Computer Vision and Pattern Recognition (CVPR). pp. 1747–1756 (2021). <https://doi.org/10.1109/CVPR46437.2021.00179>
- [15] Deschaud, J.E.: Imls-slam: Scan-to-model matching based on 3d data. In: 2018 IEEE International Conference on Robotics and Automation (ICRA). pp. 2480–2485 (2018). <https://doi.org/10.1109/ICRA.2018.8460653>
- [16] Deschaud, J.E., Duque, D., Richa, J.P., Velasco-Forero, S., Marcotegui, B., Goulette, F.: Paris-carla-3d: A real and synthetic outdoor point cloud dataset for challenging tasks in 3d mapping. Remote Sensing **13**(22) (2021). <https://doi.org/10.3390/rs13224713>, <https://www.mdpi.com/2072-4292/13/22/4713>
- [17] Dosovitskiy, A., Ros, G., Codevilla, F., Lopez, A., Koltun, V.: CARLA: An open urban driving simulator. In: Levine, S., Vanhoucke, V., Goldberg, K. (eds.) Proceedings of the 1st Annual Conference on Robot Learning. Proceedings of Machine Learning Research, vol. 78, pp. 1–16. PMLR (13–15 Nov 2017), <https://proceedings.mlr.press/v78/dosovitskiy17a.html>
- [18] Fuhrmann, S., Goesele, M.: Floating scale surface reconstruction. ACM Trans. Graph. **33**(4) (jul 2014). <https://doi.org/10.1145/2601097.2601163>, <https://doi.org/10.1145/2601097.2601163>
- [19] Graham, B., van der Maaten, L.: Submanifold sparse convolutional networks (2017)

- [20] Guo, Y., Tong, X.: View-volume network for semantic scene completion from a single depth image. In: Proceedings of the Twenty-Seventh International Joint Conference on Artificial Intelligence, IJCAI-18. pp. 726–732. International Joint Conferences on Artificial Intelligence Organization (7 2018). <https://doi.org/10.24963/ijcai.2018/101>, <https://doi.org/10.24963/ijcai.2018/101>
- [21] Hoppe, H., DeRose, T., Duchamp, T., McDonald, J., Stuetzle, W.: Surface reconstruction from unorganized points. In: Proceedings of the 19th Annual Conference on Computer Graphics and Interactive Techniques. p. 71–78. SIGGRAPH '92, Association for Computing Machinery, New York, NY, USA (1992). <https://doi.org/10.1145/133994.134011>, <https://doi.org/10.1145/133994.134011>
- [22] Kazhdan, M., Bolitho, M., Hoppe, H.: Poisson surface reconstruction. In: Proceedings of the Fourth Eurographics Symposium on Geometry Processing. p. 61–70. SGP '06, Eurographics Association, Goslar, DEU (2006)
- [23] Kazhdan, M., Hoppe, H.: Screened poisson surface reconstruction. ACM Trans. Graph. **32**(3) (jul 2013). <https://doi.org/10.1145/2487228.2487237>, <https://doi.org/10.1145/2487228.2487237>
- [24] Kolluri, R.: Provably good moving least squares. ACM Trans. Algorithms **4**(2) (may 2008). <https://doi.org/10.1145/1361192.1361195>, <https://doi.org/10.1145/1361192.1361195>
- [25] Labatut, P., Pons, J.P., Keriven, R.: Robust and efficient surface reconstruction from range data. Computer Graphics Forum **28**(8), 2275–2290 (2009). <https://doi.org/https://doi.org/10.1111/j.1467-8659.2009.01530.x>
- [26] Liao, Y., Donné, S., Geiger, A.: Deep marching cubes: Learning explicit surface representations. In: 2018 IEEE/CVF Conference on Computer Vision and Pattern Recognition. pp. 2916–2925 (2018). <https://doi.org/10.1109/CVPR.2018.00308>
- [27] Lorensen, W.E., Cline, H.E.: Marching cubes: A high resolution 3d surface construction algorithm. SIGGRAPH Comput. Graph. **21**(4), 163–169 (aug 1987). <https://doi.org/10.1145/37402.37422>, <https://doi.org/10.1145/37402.37422>
- [28] Mescheder, L., Oechsle, M., Niemeyer, M., Nowozin, S., Geiger, A.: Occupancy networks: Learning 3d reconstruction in function space. In: 2019 IEEE/CVF Conference on Computer Vision and Pattern Recognition (CVPR). pp. 4455–4465 (2019). <https://doi.org/10.1109/CVPR.2019.00459>
- [29] Metzger, G., Hanocka, R., Zorin, D., Giryes, R., Panozzo, D., Cohen-Or, D.: Orienting point clouds with dipole propagation. ACM Trans. Graph. **40**(4) (jul 2021). <https://doi.org/10.1145/3450626.3459835>, <https://doi.org/10.1145/3450626.3459835>

- [30] Mullen, P., Goes, F., Desbrun, M., Cohen-Steiner, D., Alliez, P.: Signing the unsigned: Robust surface reconstruction from raw pointsets. *Computer Graphics Forum* **29** (07 2010). <https://doi.org/10.1111/j.1467-8659.2010.01782.x>
- [31] Newcombe, R.A., Izadi, S., Hilliges, O., Molyneaux, D., Kim, D., Davison, A.J., Kohi, P., Shotton, J., Hodges, S., Fitzgibbon, A.: Kinectfusion: Real-time dense surface mapping and tracking. In: 2011 10th IEEE International Symposium on Mixed and Augmented Reality. pp. 127–136 (2011). <https://doi.org/10.1109/ISMAR.2011.6092378>
- [32] Oleynikova, H., Taylor, Z., Fehr, M., Siegwart, R., Nieto, J.: Voxblox: Incremental 3d euclidean signed distance fields for on-board mav planning. In: 2017 IEEE/RSJ International Conference on Intelligent Robots and Systems (IROS). pp. 1366–1373 (2017). <https://doi.org/10.1109/IROS.2017.8202315>
- [33] Pan, L., Chen, X., Cai, Z., Zhang, J., Zhao, H., Yi, S., Liu, Z.: Variational relational point completion network. In: 2021 IEEE/CVF Conference on Computer Vision and Pattern Recognition (CVPR). pp. 8520–8529 (2021). <https://doi.org/10.1109/CVPR46437.2021.00842>
- [34] Park, J.J., Florence, P., Straub, J., Newcombe, R., Lovegrove, S.: Deepsdf: Learning continuous signed distance functions for shape representation. In: 2019 IEEE/CVF Conference on Computer Vision and Pattern Recognition (CVPR). pp. 165–174 (2019). <https://doi.org/10.1109/CVPR.2019.00025>
- [35] Peng, S., Niemeyer, M., Mescheder, L., Pollefeys, M., Geiger, A.: Convolutional occupancy networks. In: Computer Vision – ECCV 2020: 16th European Conference, Glasgow, UK, August 23–28, 2020, Proceedings, Part III. p. 523–540. Springer-Verlag, Berlin, Heidelberg (2020)
- [36] Roldao, L., de Charette, R., Verroust-Blondet, A.: 3d semantic scene completion: a survey. *CoRR* **abs/2103.07466** (2021), <https://arxiv.org/abs/2103.07466>
- [37] Roldão, L., de Charette, R., Verroust-Blondet, A.: Lmscnet: Lightweight multiscale 3d semantic completion. In: 2020 International Conference on 3D Vision (3DV). pp. 111–119 (2020). <https://doi.org/10.1109/3DV50981.2020.00021>
- [38] Schertler, N., Savchynskyy, B., Gumhold, S.: Towards globally optimal normal orientations for large point clouds. *Comput. Graph. Forum* **36**(1), 197–208 (jan 2017). <https://doi.org/10.1111/cgf.12795>, <https://doi.org/10.1111/cgf.12795>
- [39] Song, S., Yu, F., Zeng, A., Chang, A.X., Savva, M., Funkhouser, T.: Semantic scene completion from a single depth image. In: 2017 IEEE Conference on Computer Vision and Pattern Recognition (CVPR). pp. 190–198 (2017). <https://doi.org/10.1109/CVPR.2017.28>

[40] Ummenhofer, B., Koltun, V.: Adaptive surface reconstruction with multiscale convolutional kernels. In: 2021 IEEE/CVF International Conference on Computer Vision (ICCV). pp. 5631–5640 (2021). <https://doi.org/10.1109/ICCV48922.2021.00560>

[41] Venkatesh, R., Sharma, S., Ghosh, A., Jeni, L.A., Singh, M.: DUDE: deep unsigned distance embeddings for hi-fidelity representation of complex 3d surfaces. CoRR **abs/2011.02570** (2020), <https://arxiv.org/abs/2011.02570>

[42] Wang, Y., Tan, D.J., Navab, N., Tombari, F.: Adversarial semantic scene completion from a single depth image. In: 2018 International Conference on 3D Vision (3DV). pp. 426–434 (2018). <https://doi.org/10.1109/3DV.2018.00056>

[43] Yang, G., Huang, X., Hao, Z., Liu, M.Y., Belongie, S., Hariharan, B.: Pointflow: 3d point cloud generation with continuous normalizing flows. In: 2019 IEEE/CVF International Conference on Computer Vision (ICCV). pp. 4540–4549 (2019). <https://doi.org/10.1109/ICCV.2019.00464>

[44] Yuan, W., Khot, T., Held, D., Mertz, C., Hebert, M.: Pcn: Point completion network. In: 2018 International Conference on 3D Vision (3DV). pp. 728–737 (2018). <https://doi.org/10.1109/3DV.2018.00088>

[45] Zhang, J., Zhao, H., Yao, A., Chen, Y., Zhang, L., Liao, H.: Efficient semantic scene completion network with spatial group convolution. In: Ferrari, V., Hebert, M., Sminchisescu, C., Weiss, Y. (eds.) Computer Vision – ECCV 2018. pp. 749–765. Springer International Publishing, Cham (2018)

[46] Zhang, P., Liu, W., Lei, Y., Lu, H., Yang, X.: Cascaded context pyramid for full-resolution 3d semantic scene completion. In: 2019 IEEE/CVF International Conference on Computer Vision (ICCV). pp. 7800–7809 (2019). <https://doi.org/10.1109/ICCV.2019.00789>

[47] Zhou, Y., Shen, S., Hu, Z.: Detail preserved surface reconstruction from point cloud. Sensors **19**(6) (2019). <https://doi.org/10.3390/s19061278>, <https://www.mdpi.com/1424-8220/19/6/1278>

[48] Zwicker, M., Pfister, H., van Baar, J., Gross, M.: Surface splatting. In: Proceedings of the 28th Annual Conference on Computer Graphics and Interactive Techniques. p. 371–378. SIGGRAPH '01, Association for Computing Machinery, New York, NY, USA (2001). <https://doi.org/10.1145/383259.383300>, <https://doi.org/10.1145/383259.383300>

[49] Öztireli, A.C., Guennebaud, G., Gross, M.: Feature preserving point set surfaces based on non-linear kernel regression. Computer Graphics Forum **28**(2), 493–501 (2009). <https://doi.org/https://doi.org/10.1111/j.1467-8659.2009.01388.x>